14 March 1938

NRL Report H-1432

FR-1432

NAVY DEPARTMENT
BUREAU OF ENGINEERING

Report on

The Brightness of the Twilight Sky and the Density of the Atmosphere to about 60 km.

NAVAL RESEARCH LABORATORY
ANACOSTIA STATION
Washington, D.C.

Number of Pages: Text - 14 Tables - 2 Figures - 11

Authorization: Director, Naval Research Laboratory, and Bu.C&R let. S94-(8)-(1)(ME) of 4/7/37.

Prepared by: _____
E.O. Hulburt, Principal Physicist,
Superintendent, Physical Optics Division.

Approved by: _____
H.M. Cooley, Captain, U.S. Navy,
Director.

Distribution:
BuC&R (2)
BuEng (1)
Hydrographer (1)
Naval Observ. (1)

vhw

TABLE OF CONTENTS

APPENDICES

ABSTRACT

With a calibrated Macbeth illuminometer measurements were made of i_z the brightness of the zenith sky and of i_g the energy flux across a vertical plane from the twilight horizon for the depression θ of the sun below the horizon from 0° to 13°. For clear sky conditions the i_z,θ and i_g,θ curves did not change with the season from October, 1937, to April, 1938, and were the same for evening and morning twilight. Calculation from the Rayleigh theory of molecular scattering and the observed i_z and i_g data showed that within $\pm$ 30 percent the densities of the atmosphere from sea level to about 60 km were those of the density-height relation known to 20 km and extrapolated for a temperature of 218° K. It follows that the temperature of the twilight temperate zone atmosphere is 218° $\pm$ 15° K from 20 to 60 km. The influence of secondary scattering, determined from i_g, although small for small values of θ increased rapidly with θ to such an extent that the twilight zenith sky brightness measures gave no indication of the distribution of density above about 60 km.

INTRODUCTION

In a recent experiment[1] measurements were made of the brightness of a powerful searchlight beam directed upward from which were derived values of the density of the atmosphere to a height of about 22 km. To reach higher

---

1 Hulburt, JOSA 27, 377 (1937).

---

altitudes the illumination of sunlight, which is many times brighter than that of a searchlight, may be used. It is only necessary to measure the brightness of the zenith sky during twilight in order to derive, after proper corrections are made, information about the density of the atmosphere to considerable heights. This has been attempted by Fessenkoff[2] and by Link[3] who made sky brightness measurements for θ from about 6° to 18°, θ being the angle of the sun below the horizon[4]. They concluded that their measurements indicated

---

2 Fessenkoff, Astrophysical Observatory, Moscow, Publications, 2, 113 (1923) (Résumé in French, pages 113-123; complete paper in Russian, pages 7-113).

3 Link, C.R. 199, 303 (1934); 200, 78 (1935)

4 Measures of twilight sky brightness are recorded by Kimball and Thiessen, Monthly Weather Review, 44, 614 (1916);

by Bauer, Danjon and Langevin, C.R. 172, 2115 (1924);

by Dufay, Bulletin Observatoire de Lyons, 10, No. 9 (1928);

and by Smart, Mon.Not.Roy.Ast.Soc. 93, 441 (1932-33).

---

atmospheric densities in the region from 50 to 150 km above sea level much greater than those obtained by simple extrapolation of the density-height relation observed from sea level to 20 km. The conclusion was based on the assumption that effects of secondary scattering were negligible, in contrast to the view expressed by others[4] that secondary scattering may play a preponderating role at the end of twilight. The conclusion appeared strange and the assumption open to question. A further investigation seemed desirable, since the method is the only one yet suggested of obtaining direct knowledge of upper air densities and since no measures were available in absolute units suitable for theoretical calculation; also there were no data from which the secondary scattering might be evaluated. As described below the brightness of the zenith sky and of the secondary scattering have been determined for θ from 0° to 13°. The results show that the densities of the atmosphere from sea level to about 60 km are those of the density-height relation known to 20 km extrapolated for a temperature of 218° K. The influence of secondary scattering although small for small values of θ increases rapidly with θ to such an extent that zenith sky brightness measurements give no trustworthy indication of the distribution of density above 60 km.

The plan of the present investigation was simple. Let A and S, Fig. 1, be the positions of the observer and the sunset or sunrise point, respectively,

for a depression of the sun θ. AH is the observer's horizon and Z his zenith. The region EHF is the twilight glow which the observer sees in the western sky after sunset, or in the eastern sky after sunrise. The brightness i_z of the zenith sky above the observer is the total of all the light scattered to him by the atmosphere along ABZ. In the region ZB the air is illuminated by the direct light of the sun i and in the region BA by the light of the twilight glow i_g. Measurements were made of i_z and i_g.

Denote the downward scattered light from ZB and BA by i_p and i_m, respectively. Then

$$i_z = i_p + i_m. \tag{1}$$

The molecular density n of the atmosphere to great heights was assumed. From n together with i and i_g, respectively, i_p and i_m were calculated from the Rayleigh theory of molecular scattering. Their sum was compared with the observed values of i_z to determine the correctness of the assumed values of n.

EXPERIMENTAL

Brightness measurements were made visually with a Macbeth Illuminometer, Leeds and Northrup Company, equipped with a blue filter over the photometer lamp. The blue filter, selected by trial, rendered the field of the instrument approximately the same color as the sky. The color match, although satisfactory, was not perfect, the illuminometer field being a little greener than the zenith sky. In more detail, as the sun progressed below the horizon the zenith sky appeared at first a little purpler than the field, then about the same color as the field, and finally bluer than the field; this indicated that the spectral distribution of the zenith sky light changed slightly with θ during the twilight period. Curve 1, Fig. 2, is the transmission curve of the blue filter and curve 2 is the spectral energy curve of the illuminometer lamp through the blue filter. Curve 3 is the spectral energy curve of sunlight outside of the atmosphere and curve 4 the spectral energy curve of sunlight scattered by the air molecules calculated from curve 3 by means of the Rayleigh scattering equation (6.9). Curve 4 is approximately the spectral energy curve of the zenith sky during twilight, and indicates a light more blue or more purple in tint than that of curve 2. Multiplying the curves by the visibility curve of the eye yielded two curves of similar contour in accord with the observed color match.

The illuminometer was calibrated by means of a standard tungsten lamp burning at a known temperature*; multiplying the illuminometer readings by the calibration factor gave the energy flux from the illuminated region. It does not seem necessary to describe the details of the calibration here in spite of the fact that all of the quantitative results depended entirely on it. The field of view of the illuminometer was a cone of about 4° angular diameter. By means of three neutral filters a range of intensity of 10^6 could be covered. In the case of the zenith sky the illuminometer was pointed vertically upward; the measurement gave i_z, the energy flux from the sky in ergs sec^{-1} per unit solid angle. In the case of the twilight glow measurements were made of the brightness of a white plaque of diffuse reflectivity 0.8 held in a vertical plane facing the eastern or western horizon over the sun; the measurements led to i_g erg cm^{-2} sec^{-1}, the flux of energy in an approximately horizontal direction at the observer from the twilight glow. Readings were taken at known times usually about 1 minute apart. From the time and the latitude and longitude, θ was calculated from astronomical formulae, θ being the depression of the sun, i.e., the angle between a plane tangent to the earth at the observer and a line joining the centers of the earth and sun. Neglecting atmospheric refraction the altitude h of the boundary of the earth's shadow above the observer, i.e., AB of Fig. 1, is given by

$$h = r (\sec \theta - 1) , \qquad (2)$$

where r is the radius of the earth.

All observations were made from a hill on the edge of the Potomac River. During many periods of clear sky from October 1937 to April 1938, i_z was observed throughout morning and evening twilight for θ from 0° to 13°, or h

* The lamp was standardized at the National Bureau of Standards by Dr. H.T. Wensell.

from 0 to 160 km. For $\theta > 13^{\circ}$ i_z was too small to be readily measured with the illuminometer. Although the brighter stars were beginning to be visible at $\theta = 12^{\circ}$ there was considerable daylight illumination in the zenith sky and hence the measurements were not affected by relatively faint luminous apparitions as stars, the zodiacal light and the light of the night sky. There was no disturbing artificial illumination. A few series of values of i_z erg sec^{-1} per unit solid angle are shown by dots plotted as $\log_{10} i_z$ against θ in Fig. 3; the complete series of values were too numerous to be put in a single figure. The average of the dots is shown by the i_z curve. It is seen that individual readings rarely departed from the average by as much as 40 percent; the curve was considered to be correct within about $\pm$ 30 percent as far as instrumental readings were concerned. The values of h from (2) corresponding to θ are also marked on Fig. 3.

The i_z, θ curve was the same for evening and morning twilight and did not change with the season from October 1937 to April 1938 for clear sky conditions. The march of i_z with θ was a consistent and reproducible phenomenon and was repeated day after day with numerical precision (within $\pm$ 30 percent). In accord with theory, as discussed later, it was not affected by a heavy bank of clouds rising over the sunset (or sunrise) sky nearly to the zenith as long as the zenith sky remained uncovered. It remained the same when observed through a hole through clouds in an otherwise completely overcast sky. When the sky was noticeably hazy i_z was usually below its clear sky value. On the whole when the twilight zenith sky appeared to the eye to be free from haze and clouds the i_z values were those of the curve of Fig. 3, and when the sky was visibly impure the i_z values departed from those of the curve. However, measurements of i_z accurate to a few percent would undoubtedly reveal variations due to visually imperceptible meteorological influences.

In the case of the i_g measurement, just as for i_z, a close but not exact color match was obtained. The color of the white plaque illuminated by the twilight glow was whiter than the photometer lamp through the blue filter for $\theta < 3^{\circ}$ and slightly bluer for $\theta > 5^{\circ}$. This was due to the color change of i_h with θ; i_h at first was whiter than the blue sky because of the red, orange, green, and blue sunset (or sunrise) arcs in the west (or east) and became bluer with increasing θ.

A few of the observed values of i_g erg cm^{-2} sec^{-1} are plotted as $\log_{10} i_g$ against θ in Fig. 3 for a clear and cloudless eastern or western sky; the average of all of the values of i_g is given in the smooth curve. No differences in i_g for sunset or sunrise conditions were observed, and no change with the season from October, 1937, to April, 1938. Only values of i_g for clear sky conditions were recorded, for clouds or haze over the twilight glow EHF, Fig. 1, rendered the values of no meaning in the present investigation. As illustrated in Fig. 3 the i_g points showed on the whole more scatter than the i_z points, probably because of the effects of haze or clouds over the twilight glow below the horizon of the observer and hence unnoticed. The usual routine consisted in recording i_g and i_z at alternate minutes during the twilight period. Since conditions of a clear zenith sky were more frequent than those of a clear twilight glow sky more values of i_z than of i_g were obtained.

A third series of observational data, necessary to the determination of i_m, consisted in the approximate angular dimensions of the twilight glow EHF, Fig. 1, as viewed from A. The data are given in the curves of Fig. 4. The brightest region of the twilight glow was about 5° above the horizon over the

sun for $\theta < 9^{\circ}$; each curve of Fig. 4 gives for a specified θ the contour in the sky where the brightness was about 1/3 the maximum brightness. For $\theta > 2^{\circ}$ more than 2/3 of i_g came from the region of the sky embraced by each curve. For $\theta < 2^{\circ}$, i.e. for the sun below and near to the horizon, the twilight glow spread over the entire sky and the curves were uncertain.

CALCULATIONS

The molecular density n of the atmosphere at high levels was obtained by extrapolation of the n,z relation observed in lower levels, z being the altitude above sea level. In Table 1 are given the values of n derived[5] from Humphreys'[6] tabulations based on average European observations of the temperatures and pressures to about 20 km. The values of $\log_{10}n$ are plotted as dots

---

5 Loc. cit. Ref. 1, Table 2.

6 Humphreys, Physics of the Air, 2nd Ed., page 74 (1929).

---

against z in Fig. 5. Humphreys gives two tables of atmospheric density, one for summer and one for winter; they differ by only 8 and 16 percent at z = 20 and 40 km, respectively, and would be barely distinguishable from the average dots on the scale of Fig. 5. From about 11 to 20 km the observed temperature was about 218° K and the dots fell on a straight line. Extending the line to high levels yielded the extrapolated values of n, shown in Table 1 for $z > 20$ km, assuming that throughout the high levels t = 218° K and the atmospheric composition was the same as at sea level. The curve of Fig. 5 is made up approximately of two straight lines, given by

$$n = n_o e^{-pz} , \tag{3}$$

where $p = 1.11 \times 10^{-6}$ and 1.54×10^{-6} below and above 10 km, respectively. For an isothermal atmosphere

$$p = mg/kt , \tag{3.1}$$

m being the mass of the average air particle, g the acceleration of gravity at the height z and k the Boltzman constant.

It is assumed that (3) is approximately valid to heights which, although relatively great, are small with respect to the radius of the earth. Then the total number n_1 of molecules in a vertical column above z is from (3)

$$n_1 = \int_z^\infty n\,dz = n/p. \tag{3.2}$$

A more rigorous extrapolation would take into account the curvature and rotation of the earth and other factors; however, it would differ but little from (3.2) for $z < 300$ km.

If a beam of unpolarized light of intensity i_λ erg cm^{-2} sec^{-1} and wavelength λ passes through a gas of refractive index μ_λ and molecular density n, the intensity $i_{s\lambda}$ of the light scattered per unit solid angle at an angle ϕ to the beam is

$$i_{s\lambda} = i_\lambda \, 2\pi^2 \, (\mu_\lambda - 1)^2 \, (1 + \cos^2 \phi)/n\lambda^4 \, . \qquad (5)$$

(5) is derived from the Rayleigh[7] theory of scattering by particles small with respect to λ. Integrating (5) over a sphere gives the Rayleigh expression for β_λ the attenuation due to scattering,

$$\beta_\lambda = 32\pi^3 \, (\mu_\lambda - 1)^2 \, / \, 3 \, n\lambda^4 \, . \qquad (6)$$

Now

$$\mu_\lambda - 1 = \alpha_\lambda \, n \, , \qquad (6.3)$$

where α_λ is a function of λ . α_λ has been measured[8] for air throughout the wave-length region from 2000 to 10000 A. Substituting (6.3) in (5) yields

$$i_{s\lambda} = i_\lambda 2\pi^2 n\alpha_\lambda^2 \, (1 + \cos^2 \phi)/\lambda^4 \, , \qquad (6.5)$$

which expresses the scattered intensity explicitly in terms of the molecular density n. Similarly, putting (6.3) into (6) gives

$$\beta_\lambda = 32\pi^3 \alpha_\lambda^2 \, n/3\lambda^4 \, . \qquad (6.6)$$

---

7 Rayleigh, Phil.Mag. 51, 107, 274 (1871); 47, 375 (1899).

8 Meggers and Peters, Bul.Nat.Bur.Stand. 14, 731 (1918).

In the case of scattering at right angles to the beam ϕ is 90° and (6.5) becomes

$$i_{s\lambda} = i_\lambda \, 2\pi^2 \, n\alpha_\lambda^2 \, / \lambda^4 \, , \qquad (6.9)$$

or

$$i_{s\lambda} = i_\lambda \, s_\lambda \, n \quad \text{where} \quad s_\lambda = 2\pi^2 \alpha_\lambda^2 \, / \lambda^4 \, . \qquad (7)$$

Curve 3, Fig. 2, is the spectral energy curve of sunlight outside of the atmosphere[9] and curve 4, calculated from curve 3 and (6.9), is the spectral energy of sunlight scattered by the atmosphere; curve 4 refers approximately to the twilight sky.

---

9 Smithsonian Physical Tables, page 608 (1933)

If the light of total intensity i is distributed over a spectral region the total scattered light i_s is found by integrating (7) over the region. Then

$$i_s = \int i_{s\lambda}\, d\lambda = \int i_\lambda\, s_\lambda\, n\, d\lambda = n \int i_\lambda\, s_\lambda\, d\lambda ,$$

which may be written

$$i_s = i\, n\, \frac{\int i_\lambda\, s_\lambda\, d\lambda}{\int i_\lambda\, d\lambda} \equiv i\, n\, s , \qquad (7.2)$$

where s is the ratio of the integrals. For sunlight outside of the atmosphere the solar constant, i.e., the flux in all wave-lengths, is 1.36×10^6 erg cm^{-2} sec^{-1}, the flux i in the visible spectrum from 400 to 720 $\mu\mu$ is 6.83×10^5, and $s = 3.42 \times 10^{-28}$ as determined from the areas under curves 3 and 4, Fig. 2. s is the fraction of the energy in the visible wave-lengths of sunlight scattered at right angles per unit solid angle per air molecule.

A calculation of i_p requires the determination of the spectral energy distribution of the sunlight at each height z in the region BZ, Fig. 1. This in turn requires consideration of the effects of the finite angular size of the sun seen from the earth and of the refraction and attenuation by the atmosphere of solar rays passing over the sunset point S, Fig. 1, to BZ.

The radius of the solar disk subtends an angle δ = 16 minutes of arc at the earth. Neglecting, for the moment, atmospheric refraction and attenuation, let MS and NS, Fig. 6, be lines from the upper and lower edges of the solar disk, respectively, tangent to the earth; BS is the line from the center of the sun tangent to the earth. Since we deal with the distance AS always less than 13°, MZ is approximately vertical and perpendicular to BS. Above N the intensity is that of full sunlight i_o; below M the intensity is zero, this being the region of shadow. Let y be the angular distance measured up from M; the distance MN is 2δ. The intensity i of the sunlight in the penumbra at any point between M and N is

$$i = i_o \left\{ \pi\delta^2/2 + (y-\delta)\left[\delta^2 - (y-\delta)^2\right]^{1/2} + \delta^2 \sin^{-1}(y-\delta)/\delta \right\} / \pi\delta^2 \qquad (7.3)$$

i from (7.3) is plotted in curve 1, Fig. 7.

The intensity i_s = ins of the light scattered downward was calculated from (7.2) for each value of y, or corresponding level z, and is plotted in curve 2, Fig. 7. Then

$$i_p = \int_M^\infty i_s\, dz \qquad (7.4)$$

and is given by the area under curve 2.

Suppose that the sun were a point source concentrated at the center of the sun and giving the same i_o. There is then no penumbra; above B, Fig. 6, the intensity is i_o and below B is zero. The intensity $i'_s = i_o n s$ of the downward scattered light at each level z was calculated from (7.2) and is plotted in curve 3, Fig. 7. In this case

$$i_p = \int_B^\infty i'_s \, dz \tag{7.5}$$

and is given by the area under curve 3. Calculation shows that (7.4) is about 2 percent greater than (7.5) for $\theta = 4^\circ$ and about 6 percent greater for $\theta = 11^\circ$. In brief, (7.5) is approximately the same as (7.4). Therefore, in any calculation of i_p accurate to about 5 percent the sun may be taken as a point source at its center. The result simplifies subsequent calculations very much.

Attentuation of the rays of the sun by the atmosphere is assumed to be due only to scattering by air molecules according to the Rayleigh equation (6.6). Haze will produce an additional degradation of the rays which pass sufficiently close to the earth. The amount of haze present in any particular case was not known and its effects can not be calculated, but as shown later they are not important as long as there is not too much haze. Referring to Fig. 1, let SB be x and BA be z; let r be the radius of the earth. Then $x^2 = (r + z)^2 - r^2$, and since z is much less than r, $x \cong (2rz)^{1/2}$. Differentiating and multiplying each side of the equation by n of (3) gives

$$n dx = (r/2)^{1/2} \, n_o e^{-pz} \, z^{-1/2} \, dz \tag{7.9}$$

Let n_2 be the total number of air molecules in the path of a solar ray which passes entirely through the atmosphere at a point of nearest approach to the earth where the molecular density is n_o and the height z_o. Then

$$n_2 = 2 \int_{z_o}^\infty n \, dx$$

From (7.9)

$$\begin{aligned} n_2 &= n_o (2r)^{1/2} \int_{z_o}^\infty z^{-1/2} \, e^{-pz} \, dz \quad , \\ &= n_o (2r/p)^{1/2} \int_{z_o}^\infty (pz)^{-1/2} \, e^{-pz} \, dpz \quad , \\ &= n_o (2r/p)^{1/2} \, \Gamma (1/2) \quad , \\ &= n_o (2\pi r/p)^{1/2} \end{aligned} \tag{8.4}$$

By means of (8.4), (6.6) and curve 3, Fig. 2, the spectral energy curves were calculated of solar rays after passing through the atmosphere at various distances z_o of closest approach to the surface of the earth. The curves are given in Fig. 8; the curve for $z_o = \infty$ is the same as curve 3, Fig. 2, for sunlight outside of the atmosphere. Because of the change in the slope of the curve of Fig. 5 at 10 km a minor numerical approximation entered into the calculation of the curves for $z_o < 10$ km. The curves are the numerical representation of the reddening of the twilight sky near the horizon. Multiplying each ordinate of the curves of Fig. 8 by s_λ of (7) produced the family of curves of Fig. 9, which are the spectral energy curves of the light of the respective curves of Fig. 8 scattered by air molecules.

Solar rays passing into the atmosphere are bent downward by atmospheric refraction. The total deviation of the ray from infinity, i.e., outside of the atmosphere to closest approach z_o is proportional to the atmospheric density at z_o, and for the ray tangent to the surface of the earth, i.e., $z_o = 0$, is 68 minutes of arc. The height of any point of a ray is determined from the ray paths[10].

---

10 The exact paths of rays through the atmosphere have been calculated by J. Sweer of this Laboratory. His work will appear in a separate report.

From the foregoing results i_p was calculated for various values of θ. The details are tedious and obvious and may be described by giving one example. Consider the calculation of i_p for $\theta = 6^\circ\ 25'$ corresponding to h = 40 km from (2). The ray of original intensity 6.83×10^5 erg cm^{-2} sec^{-1} for which z_o = 10 km is reduced by absorption to $0.206 \times 6.83 \times 10^5 = 1.41 \times 10^5$ (from Fig. 8), is bent downward 17.6' by refraction, is spread out by dispersion, and finally passes above A, Fig. 1, with an intensity 9.20×10^4 erg cm^{-2} sec^{-1} at an altitude of 46.6 km where $n = 2.98 \times 10^{16}$ air molecules cm^{-3}. Then from (7.2) and Fig. 9 $i_{pz} = 6.28 \times 10^{-7}$ erg sec^{-1}, where i_{pz} erg sec^{-1} denotes the downward scattered energy per unit solid angle per cm^3 of air at a height z. The value is plotted at the point marked 10 on the i_{pz}, z curve for $\theta = 6^\circ\ 25'$ of Fig. 10. Similarly, the other points of the curve were determined for the rays of various values of z_o marked on the curve. i_p is given by the area under the curve or

$$i_p = \int_{28.5}^{\infty} i_{pz}\, dz\ , \qquad (9)$$

which is 1.82 erg sec^{-1}. The spectral energy curve of i_p being a composite of the curves of Fig. 9, is slightly more intense in the longer wave-lengths than curve 4, Fig. 2.

In like manner the other i_{pz}, z curves of Fig. 10 were determined and the values of i_p calculated from (9) as a function of θ. The i_p, θ curve is given in curve 2, Fig. 10 and the values are tabulated in column 5, Table 2. For comparison the observed average i_z curve of Fig. 3 is plotted in curve 1, Fig. 10; within the error of experiment it agrees with the theoretical curve 2 for θ from 0° to about 6°, or h from 0 to about 40 km. The result establishes the correctness of the values of n of Table 1 and Fig. 5 to about 40 km.

The small departure between curves 2 and 1 for θ from 2° to 5° is not regarded as of much significance. It is nearly within the variation of experiment; it may be real and attributable to slight haze below 20 km.

In order to calculate i_m from the observed values of i_g consider a point J on AB, Fig. 1. Let JGK be a tangent to the earth at G; the two points J and G "see" the same twilight glow region at and above K. Neglecting atmospheric absorption and refraction the flux i_j and i_g at J and K, respectively, from the twilight glow depend on the solid angles ω_J and ω_K subtended by the glow at J and K according to

$$i_j = i_g \quad \omega_g / \omega_j \quad . \tag{9.3}$$

ω_g and ω_j were calculated from the curves of Fig. 4 and the known values of GK and JK. i_j was then calculated for various points along AB for various values of θ. The influence of atmospheric absorption and refraction on the values of i_j is difficult to determine. An ex act calculation would require, among other unavailable data, the brightness of all portions of the twilight glow regions drawn in Fig. 4. Because the light from the twilight glow on the whole traverses less atmosphere in passing to J than in passing to G, and because of downward refraction, approximate calculation indicates that i_j of (9.3) should be increased by a factor between 2 and 6 for AJ > 20 km. Accordingly i_j for J at 10, 20, 30 and 40 km has been multiplied by 1, 2, 3 and 4, respectively. The values of i_j are not presented here.

The downward scattered light i_{mz} at J was calculated from i_j by means of (7.2) assuming, in approximate accord with observation for $\theta > 3°$, that the spectral distribution of i_j was that of curve 4, Fig. 2. On this assumption (7.2) is

$$i_{mz} = i_j \, n \, s \tag{9.4}$$

where $s = 4.78 \times 10^{-28}$. The values of i_{mz} are plotted in the lower curves of Fig. 10. i_m is given by the area under the i_{mz}, z curve, or

$$i_m = \int i_{mz} \, dz \, , \tag{9.5}$$

the integral being taken from A to B, Fig. 1. The values of i_m are in column 6, Table 2. No quantitative theory of i_g is offered here. The twilight glow arises from sunlight scattered in the atmosphere but no attempt is made to calculate i_g from the scattering formulae; a calculation would be complicated[11]. We have merely measured i_g and have calculated i_m from it; i_m arises from multiple scattering.

---

11 Raman, "Molecular Scattering of Light", 1922, page 39, indicated that he had attempted to formulate a quantitative theory of the intensity of twilight without, however, complete success.

The sum of i_p and i_m should be i_z. $i_p + i_m$ is tabulated in column 7, Table 2, and agrees within the error of experiment and calculation with the

observed values of i_z in column 3; its logarithm is plotted in curve 3, Fig. 11. The values of $i_p + i_m$ are open to two small corrections which counteract each other to some extent and hence are neglected, the one due to vertical attenuation and the other to light entering the region of i_p in addition to the direct rays of the sun. Because of atmospheric attenuation of the zenith sky light as seen by the observer, the values of $i_p + i_m$ should be decreased by about 10 percent, for from (6.6) wave-lengths 6500A and 4500 A are decreased 4 and 21 percent, respectively, in passing vertically through the atmosphere. Light other than the direct rays of the sun, such as light of the twilight glow i_g, passing into the region of i_p will increase $i_p + i_m$ by an amount considerably less than 20 percent, since the brightness of the illumination from the sky on a sunny day is only about 1/5 that from the sun. For this reason there is no entry for i_m at $\theta = 0^\circ$ in Table 2. It is much smaller than i_p, but its exact value can not be derived simply from the present measurements; it could of course be determined from an easily arranged experiment.

CONCLUSIONS

It is seen from Table 2, or Fig. 10, that i_p is much larger than i_m for $h < 60$ km, or, in other words, that the zenith sky light is mainly due to light scattered from the atmosphere lighted by the direct rays of the sun. i_p is calculated from the molecular density n above h. Therefore the agreement of $i_p + i_m$ with i_z indicates that n of Table 1 for temperate latitudes during twilight is correct within $\pm$ 30 percent for altitudes up to about 60 km. For $\theta > 8^o$, or h above 60 km, i_m is much greater than i_p; i_m is due to scattered sunlight rescattered mainly from levels below 30 km as shown by the i_m curves of Fig. 10. Therefore the twilight sky measurements lead to no information about n in levels above 60 km.

A repetition of the present investigation might be profitable, preferably with higher precision and from a mountain or other locality where a clear atmosphere prevails; possibly approximately monochromatic light could be used although this might be difficult. Polarization observations and data of the sky brightness at other points than the zenith would contribute further details of twilight phenomena. Data obtained during the long twilight of high altitudes, or during a solar eclipse might be of exceptional interest. However, in view of the rapidity of the decrease of i_p and the increase of i_m with increasing θ, it is doubtful whether twilight sky brightness measurements can yield any exact values of atmospheric densities much above 60 km. The conclusions of various writers[2, 3, 12] that twilight phenomena offer information

---

12 For example, Wegener, Lehrbuch der Physik (Müller-Pouillets) 5, 228 (1938).

---

about the atmosphere in reaches above 80 or 100 km appear to need correction, for the results of the present investigation indicate that phenomena which were thought to arise from primary scattering in relatively high levels probably arise from secondary scattering in relatively low levels.

The explanation of the small or negligible effect on the brightness of the zenith twilight sky occasioned by clouds over the sunset or sunrise horizon emerges from the curves of Fig. 10. Clouds are usually confined to heights below 8 km, and it is seen from the curves of i_p and i_m that the contribution from light which has passed within 8 km of the earth's surface is relatively small. In other words, the attenuation in even a clear atmosphere of rays of light which traverse levels below 8 km is so great that an additional opacity due to clouds is of little consequence. Similarly, haze in the lower atmosphere causes little change in the sunlight illumination of the zenith twilight sky and reduces the zenith brightness in so far as it obstructs the observer's upward view.

The experimental result that the molecular density of the atmosphere up to about 60 km is that of Table 1 within about $\pm$ 30 percent leads to knowledge of the temperature. From (3) and (3.1) t is $218^o \pm 15^o$ K from about 12 to 60 km for the twilight atmosphere of a temperate latitude. The conclusion is in agreement with the theoretical deductions of Maris[13] concerning the thermal

---

13 Maris, Terr.Mag. and Atmos.Elec. 33, 233 (1928); 34, 45 (1929).

---

state of the night atmosphere in high levels; it does not support contentions[14] of high night temperatures below 60 km.

---

14 Martyn and Pulley, Proc.Roy.Soc. 154, 455 (1936), argued that the temperature increased from about 220°K at 40 km to above 400° at 70 km.

The accuracy of the determination of n is not sufficient to throw light on the question at what altitude complete mixing of the atmospheric gases ceases and isothermal separation begins. It is known from high altitude balloon flights[15] that the proportions of nitrogen and helium at 20 km and of

---

15 Shepherd, National Geographic Society - U.S. Army Air Corps Stratosphere Flight of 1935. Technical Papers, p. 117 (1936); Regner, Nature 138, 544 (1936); Lepape and Colange, Nature 137, 459 (1936); Paneth and Glückauf, Nature 136, 717 (1935); Prokofiew and Glotzman, Nature 133, 918 (1934).

---

oxygen at 29 km are the same as at sea level within a few percent, and hence that complete mixing exists at least up to 20 km. Maris[13] has given a convincing calculation that complete mixing should prevail up to 100 km. If isothermal separation should set in at 20 km n at 40 and 60 km would be 1.5 and 6.2 percent greater than the values of Table 1 which were based on the assumption of complete mixing. The difference is too small to be revealed by the present measurements.

TABLE 1

Average temperature and molecular density of the atmosphere.

z	t	n	z	t	n
0 km	275°K	2.61×10^{19}	80 km	218°K	1.70×10^{14}
10	219°	8.60×10^{18}	90	218°	3.59×10^{13}
20	218°	1.86×10^{18}	100	218°	7.82×10^{12}
30	218°	3.95×10^{17}	110	218°	1.66×10^{12}
40	218°	8.32×10^{16}	120	218°	3.43×10^{11}
50	218°	1.77×10^{16}	130	218°	7.28×10^{10}
60	218°	3.80×10^{15}	140	218°	1.56×10^{10}
70	218°	8.03×10^{14}	150	218°	3.42×10^{9}

TABLE 2

Twilight sky data.

(1)	(2)	(3)	(4)	(5)	(6)	(7)
θ	h	i_z	i_g	i_p	i_m	$i_p + i_m$
0°	0 km	1140	436	1170	-	1170
4°34'	20	27.5	31	36.3	0.50	36.8
5°36'	30	7.41	8.7	7.9	0.43	8.3
6°25'	40	2.19	3.3	1.8	0.21	2.0
7°52'	60	0.339	0.64	8.8×10^{-2}	0.12	0.21
9°36'	80	0.0676	0.090	3.4×10^{-3}	0.063	0.066
10°9'	100	0.0398	0.051	1.4×10^{-4}	0.026	0.026
11°8'	120	0.0158	0.020	5.0×10^{-6}	0.0071	0.0071
12°2'	140	0.0076	0.010	2.1×10^{-7}	0.0049	0.0049
12°52	160	0.0040	0.005	8.3×10^{-9}	0.0024	0.0024

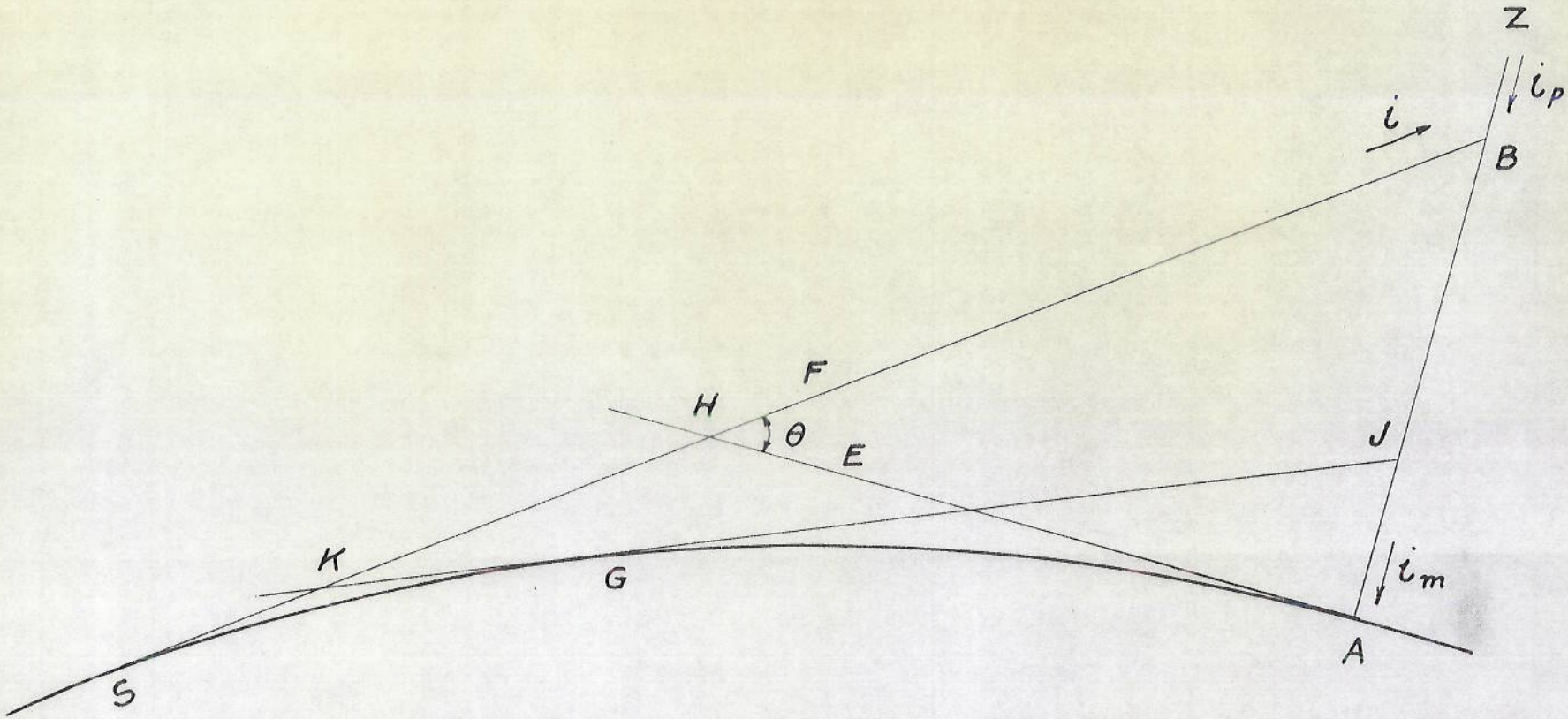

FIG. 1

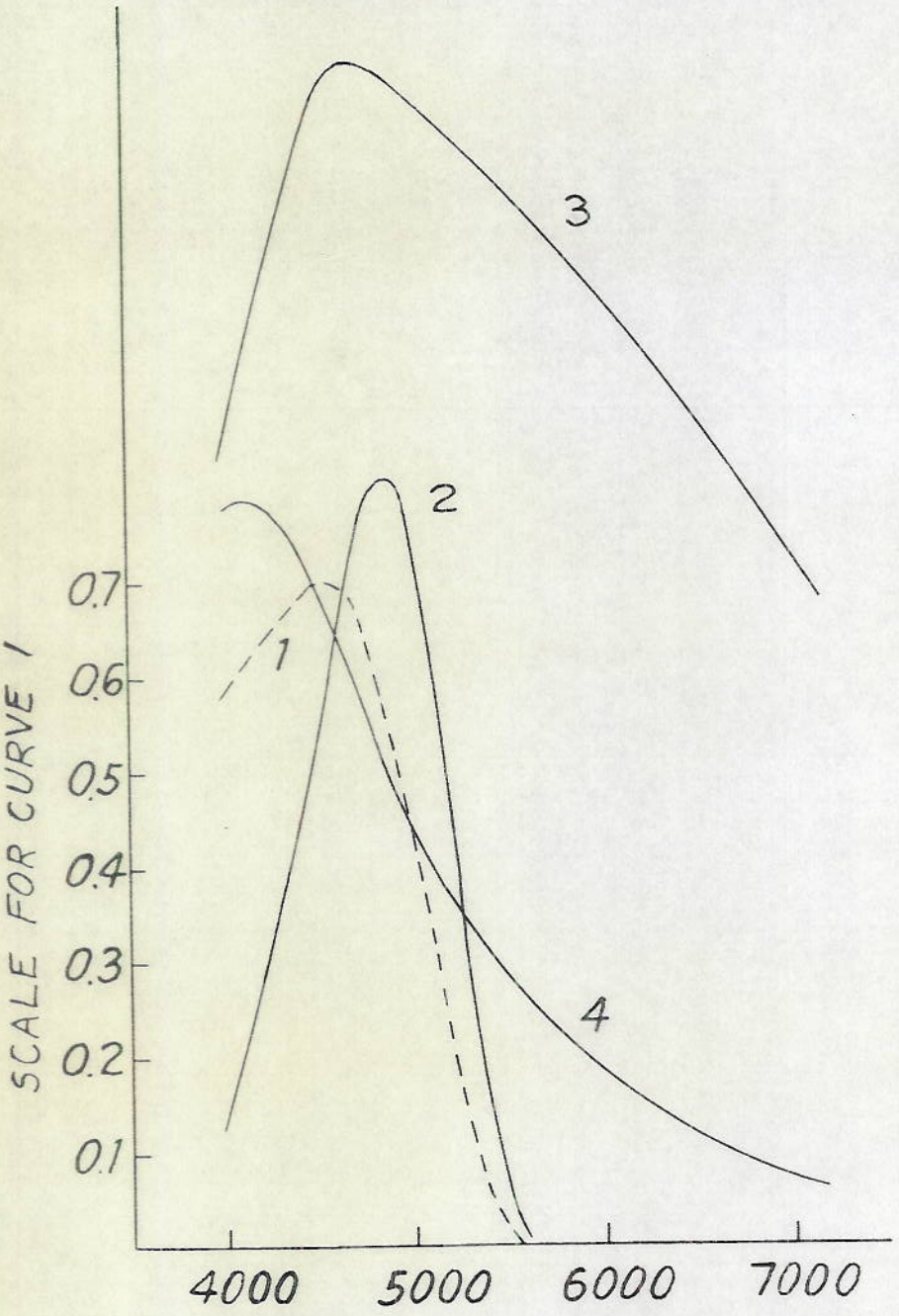

FIG. 2

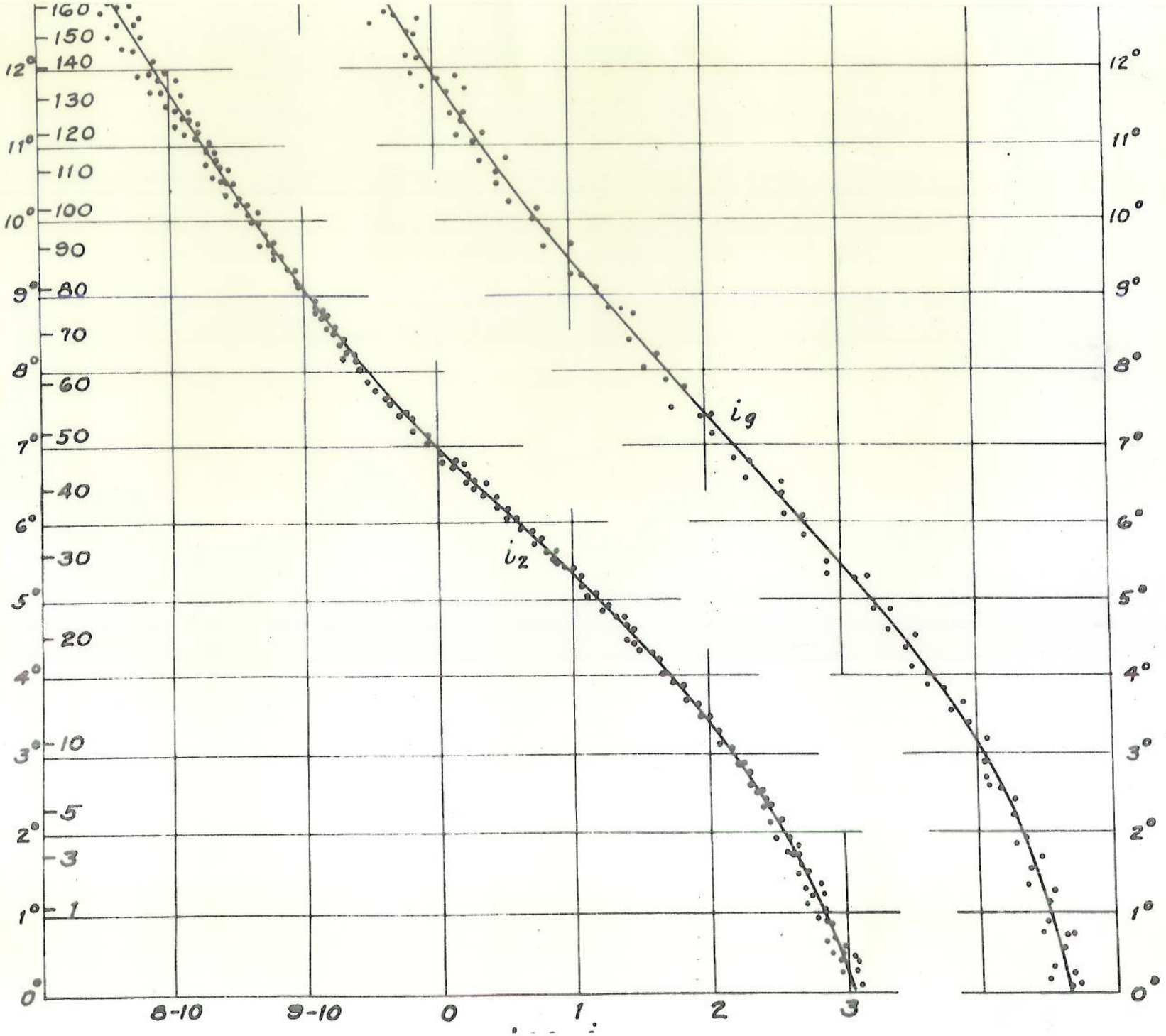
160
150
140
130
120
110
100
90
80
70
60
50
40
30
20
10
5
3
1
12°
11°
10°
9°
8°
7°
6°
5°
4°
3°
2°
1°
0°
i_g
i_z
8-10
9-10
0
1
2
3

FIG. 3

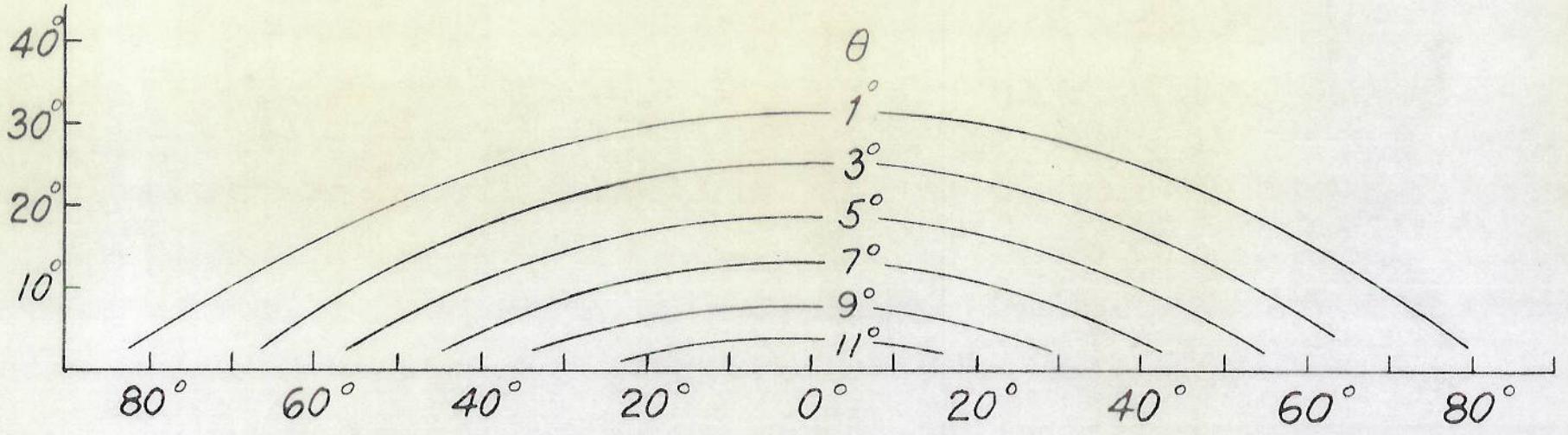

FIG. 4

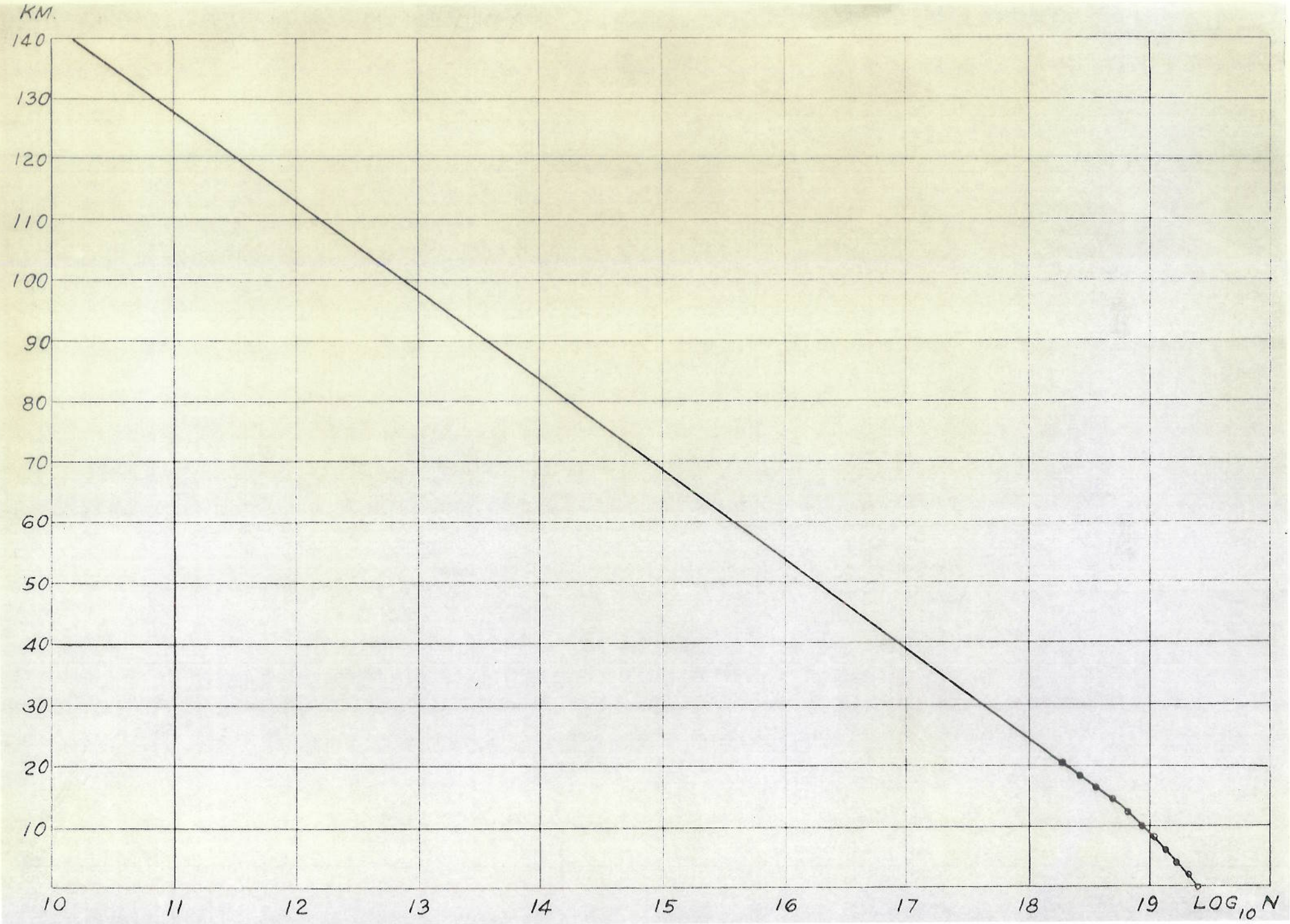
KM.
140
130
120
110
100
90
80
70
60
50
40
30
20
10
10
11
12
13
14
15
16
17
18
19
LOG10 N

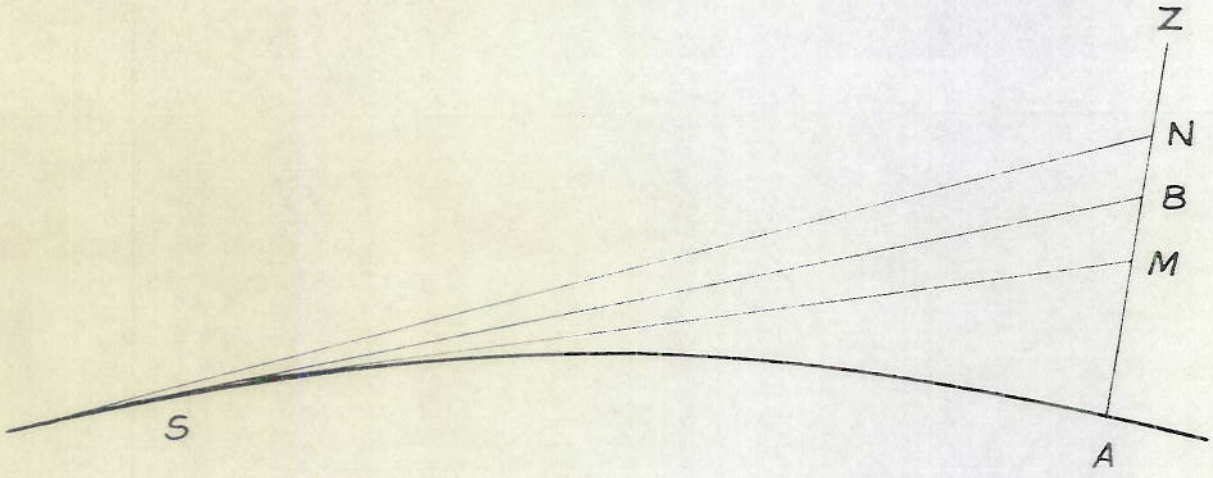

FIG. 6

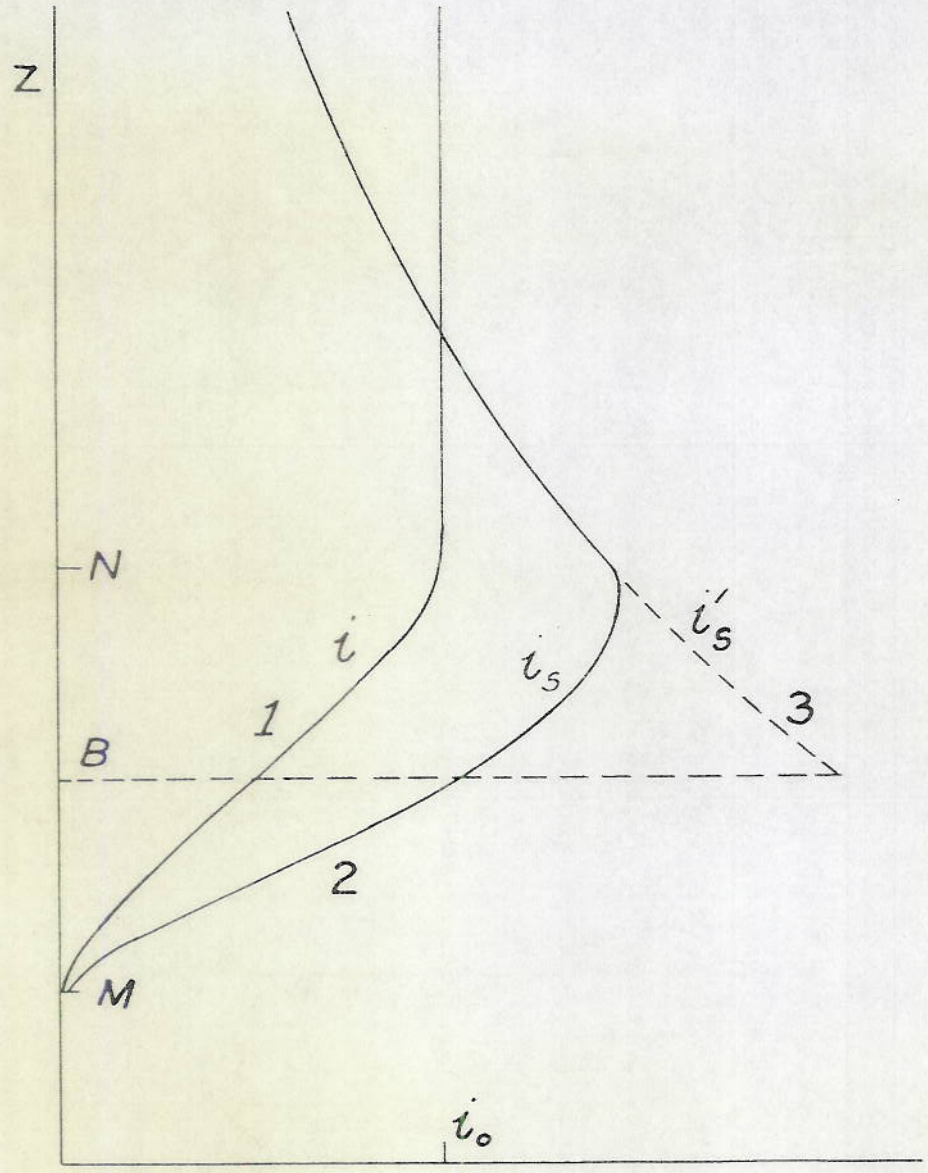

FIG. 7

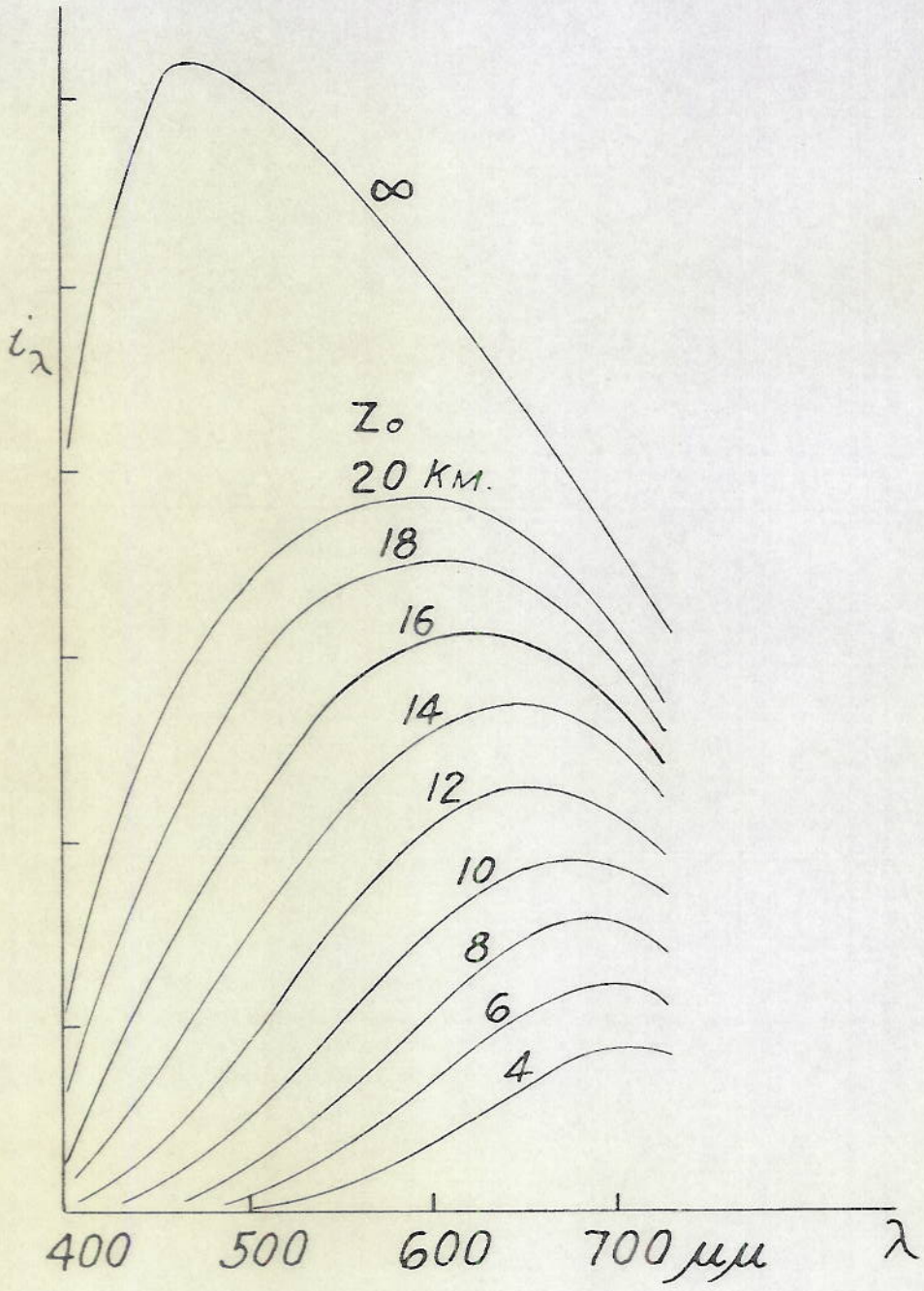

FIG. 8

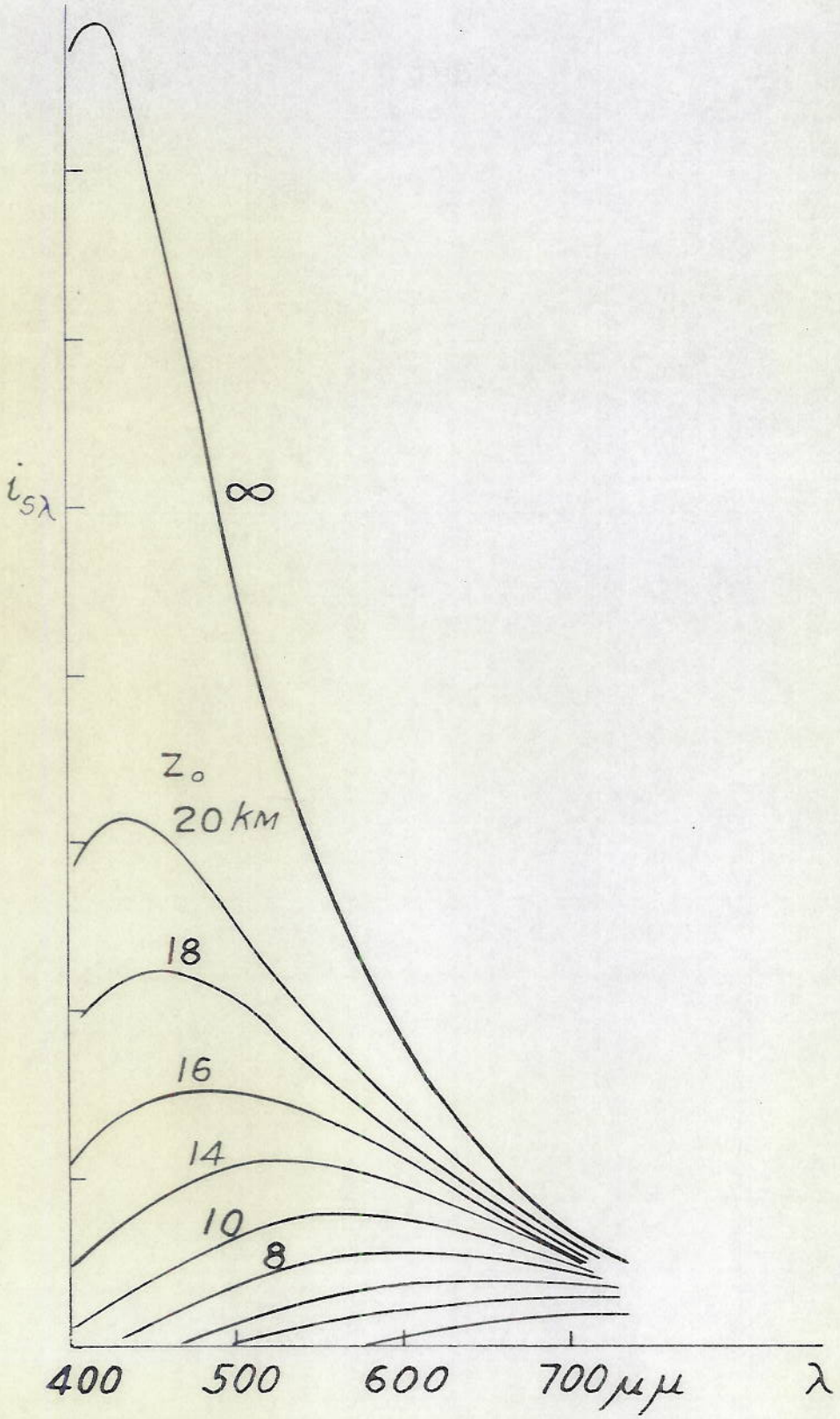

FIG. 9

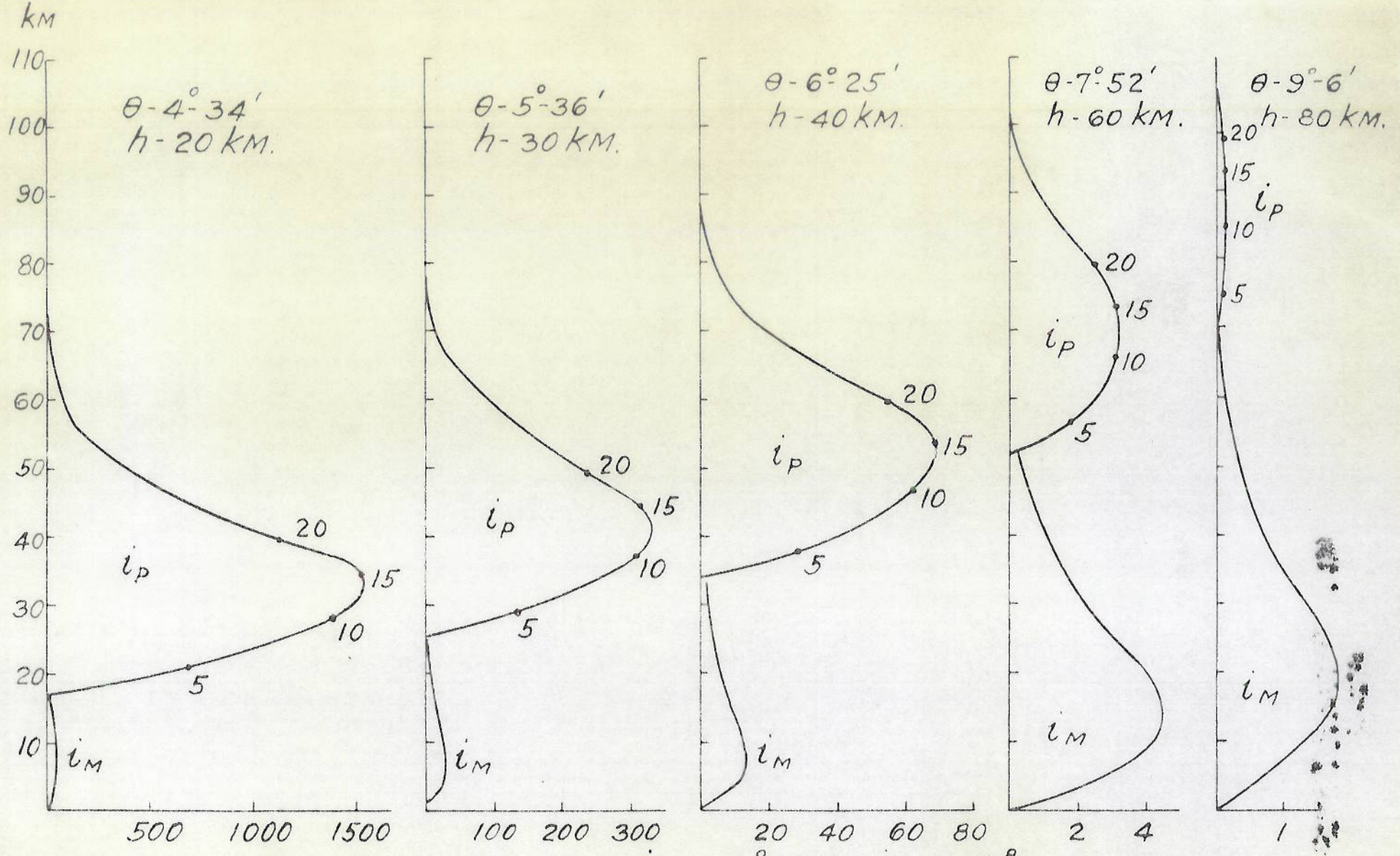
km
110
100
90
80
70
60
50
40
30
20
10
θ-4°-34'
h-20 km.
θ-5°-36'
h-30 km.
θ-6°-25'
h-40 km.
θ-7°-52'
h-60 km.
θ-9°-6'
h-80 km.
i_P
i_M
20
15
10
5
500
1000
1500
100
200
300
20
40
60
80
2
4
1
$i_{PZ} \times 10^8$ AND $i_{MZ} \times 10^8$

FIG. 10

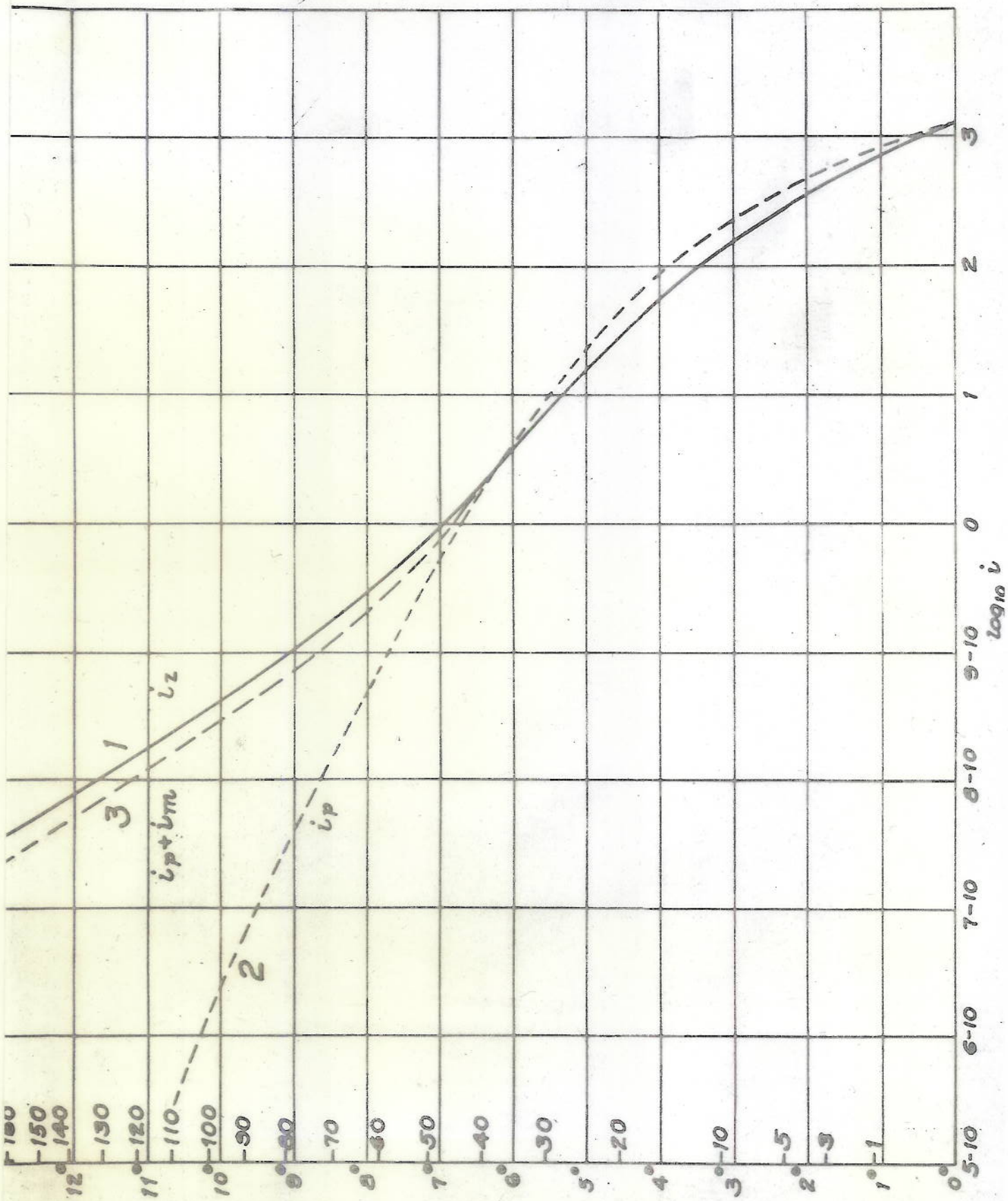

FIG. 11